J. COMBIN. MATH. COMBIN. COMPUT. 127a (2025) 4379--4394

Journal of Combinatorial Mathematics and Combinatorial Computing
www.combinatorialpress.com/jcmcc

Combinatorial Press

Personalized ceramic artwork design innovation and process parameter optimization based on 3D printing technology

Zheng Yuan[1,✉]

[1.] Zhengzhou Academy of Fine Arts, Zhengzhou, Henan, 450000, China

ABSTRACT

Ceramics have many applications, covering scientific research, medical, industrial, jewelry, etc. Ceramic materials are stable and have a silk-like touch. Ceramic 3D printing technology is based on laser curing molding as a rapid manufacturing technology. This paper proposes a personalized design strategy for ceramic artwork, determines the degree of influence of ceramic process parameters on the quality of laser 3D printed ceramic artwork by calculating the Pearson's correlation coefficient, and adopts numerical simulation to obtain the ceramic 3D printing quality data, calculates the error of the number of printed layers, and controls the quality of the printed ceramic artwork. The ceramic quality parameter optimization model is established. Five algorithms of SVR support vector regression, BP neural network, RF random forest, RBF radial basis function, and Kriging model are used to set up the relevant parameters of 3D printing, input the six ceramic process parameters that have been processed by the unified magnitude, and complete the optimization of the quality ceramic process parameters of laser 3D printing. Through the investigation and analysis of the effect of ceramic artwork design, the ceramic color designed in this paper makes the user generate positive emotions; a total of 235 positive emotions were generated, accounting for nearly 60%. The mean value of user preference for ceramic samples is analyzed. The samples with the highest user preference are sample 4, sample 6, and sample 1, and the mean values of preference are 3.425, 3.245, and 3.148, respectively.

Keywords: Numerical simulation, Ceramic quality parameter optimization, SVR support vector regression, RF random forest, personalized ceramic design

1. Introduction

3D printing technology, also known as rapid prototyping technology, was born in the late 1980s, is a new type of manufacturing and processing process, based on digital models, using powdered metals or plastics and other bondable materials, through 3D printers, layer-by-layer printing to construct the object manufacturing technology [1-4]. Due to its rapid development in the field of product design,

✉ Corresponding author.
E-mail address: 13683835853@163.com (Z. Yuan).
Received 20 February 2024; Revised 25 April 2024; Accepted 20 November 2024; Published Online 15 April 2025.
DOI: 10.61091/jcmcc127a-248

production, and application of a wide range of parts, some parts that originally need to be manufactured by traditional molds are replaced by 3D printed parts, and even the traditional molds are replaced by 3D printed molds [5-8]. Multiple 3D printing methods exist, each with its own unique applications and advantages. Due to its multiple advantages, 3D printing technology has also been used in the design and innovation of ceramic artwork [9-10].

Since China's reform and opening up, both social development and economic development have achieved better results, and at the same time, people also pay more attention to the expression of emotions. In treating the function related to ceramic artwork, people gradually begin to turn their attention to the personalization and quality of ceramic artwork [11-14]. The introduction of new technologies, new materials and new techniques, so that ceramic artwork to meet people's personalized demands become possible [15-16]. The fundamental goal of the personalized design of ceramic artwork is to take the emotional pursuit of the general public as the main object, according to people's spiritual and material needs, to take the corresponding raw materials, through the artist's use of the material, to produce ceramic artwork that can satisfy people's emotional pursuit [17-20].

This paper puts forward the personalized design strategy of ceramic artwork for the four aspects of shape, decoration, color, and material and deduces the ceramic design parameters affected by the quality of laser 3D printing technology. Numerical simulation obtains the ceramic process parameters and establishes an optimization training model. The average value of the error of the ceramic process parameters is used as the measurement accuracy standard of laser 3D printing quality to improve the 3D printing quality further. The six mined ceramic process parameter data scales are normalized, and five algorithms, namely, SVR support vector regression algorithm, BP neural network, RF random forest, RBF radial basis function, and Kriging model, are sequentially utilized to train the printed ceramic process parameters. The trained neural network was used to derive individual fitness values, solve the model, and complete the optimization of ceramic process parameters for laser 3D printing quality. A random survey analyzes factors such as color mood utility value to summarize the degree of user preference for the ceramic artwork designed in this paper.

2. Ceramic artwork personalized design

2.1. Ceramic artwork personalized design strategy

2.1.1. Individualized styling. The artistic way of ceramic artwork is mostly reflected by decoration and modeling, in which modeling is the main form of ceramic artwork in the first place. However, decoration plays a beautifying and enriching role in modeling. In all kinds of ceramic art modeling forms, the three essential elements are beauty, material technology, and functional utility; the three are interlinked and interact. According to the purpose of ceramic art and functionality, design production to meet the emotional pursuit of all kinds of audiences personalized ceramic art. The personalized ceramic art design is to meet the basic functional requirements under the premise of the skilled grasp of the technology and process, according to the characteristics of the raw materials, to achieve the “art of the material” goal so that the shape of ceramic art is more personalized.

2.1.2. Personalized decorative design. The intersection of Chinese and foreign cultures and the use of new technologies, techniques, and materials does not produce a completely new art model. In the current ceramic artwork, the most popular is the applique decoration, the audience's personalized emotional pursuit of the decoration of ceramic artwork, which has an extremely important significance.

2.1.3. Personalized color design.First, in the process of personalized design of ceramic artwork, one should pay attention to different colors. For example: “red and green color” is mainly composed of green, red, blue, and yellow; however, in all kinds of colors in red, green second, and yellow, the hue is obvious, forming a strong contrast, so that people can feel in the spirit of the level of "rich and beautiful, lively, celebratory "at the same time with obvious oriental national characteristics.

Second, in personalized decorative design, maybe pay attention to the color of the design. In the context of the continuous development of the times, color has become a special decoration, and people's daily lives, folk customs, and aesthetics are closely linked. Therefore, on the basis of ensuring the reasonable structure of ceramic artwork, the design of appropriate personalized color decoration not only plays the role of embellishing the picture but can also give people a visual impact and enjoyment, producing emotional resonance.

2.1.4. Personalized material selection. The starting point of design lies in the "material," and choosing and using the right material is always the first thing that should be paid attention to in the design of artwork. Therefore, without the personalized material, there is no way to talk about the personalization of the artwork and its function of satisfying the emotional pursuit of the audience. If you are not good at choosing good materials, you can not design a good artwork. Ceramic art is very rich in its material and is also constantly evolving. In addition, the use of synthetic or natural materials, such as metal and rattan, can often have unexpected effects.

2.2. Personalized ceramic artwork design under 3D printing technology

2.2.1. Determination of ceramic design parameters influenced by laser 3D printing quality.Laser 3D printing quality is a generalized concept affected by the ceramic process parameter settings, so the two have a direct linear relationship. The complexity of the laser 3D printing process, there are many ceramic process parameters; it is not realistic to optimize all the parameters, and not every parameter has a great impact on the laser 3D printing quality, so as long as the ceramic process parameters that have a greater impact on the quality of the ceramic process parameters can be selected. Here, the Pearson correlation coefficient is calculated to determine the degree of influence of the ceramic process parameters on the quality of laser 3D printing, so as to select the top K parameter with the greatest influence, and then take these parameters as the object to carry out optimization. The calculation formula is as follows:

$$P_j = \frac{\sum_{i=1}^{n}\left(A_{ij} - \overline{A}\right)\left(B_{ij} - \overline{B}\right)}{\sqrt{\sum_{i=1}^{n}\left(A_{ij} - \overline{A}\right)^2} \cdot \sqrt{\sum_{i=1}^{n}\left(B_{ij} - \overline{B}\right)^2}} \tag{1}$$

where P_j represents the Pearson's correlation coefficient between the j nd ceramic process parameter and the laser 3D printing quality, A_{ij} represents the j th ceramic process parameter for the i th sample, A represents the average value of the j th ceramic process parameter for all the samples, B_{ij} represents the laser 3D printing quality for the i th sample, B represents the average value of the laser 3D printing quality, and n represents the number of samples.

2.2.2. Laser 3D printing quality data acquisition.The optimization model built using data mining is essentially a nonlinear mapping relationship model between ceramic process parameters and laser 3D printing quality constructed after learning and training. The model is built by relying on each ceramic process parameter and its corresponding laser 3D printing quality data, i.e., training samples. Numerical simulation was used to obtain the data. A 50 cm × 50 cm × 50 cm square was used as the object to be printed, and the laser 3D printing process was simulated according to the numerical simulation program to obtain the virtual laser 3D printed square object, and then the multilayer printing error in three directions between the square printing result and the expectation was measured as a measure of the laser 3D printing quality. The calculation formula is as follows:

$$\Delta C=\sqrt{(I_x-\hat{I}_x)^2+(I_y-\hat{I}_y)^2+(I_z-\hat{I}_z)^2} \tag{2}$$

Wherein, ΔC represents the printing error, I_x, I_y, I_z represents the square print size in the x, y, and z directions, and $\hat{I}_x$, $\hat{I}_y$, $\hat{I}_z$ represents the square expected print size in the x, y, and z directions.

Since the printing is done one layer at a time, in order to further precise the measurement accuracy of the laser 3D printing quality, the error of each layer is calculated according to the above formula (2), and then the average value of the error is calculated, which is used as the measurement standard of the laser 3D printing quality. The calculation formula is as follows:

$$\Delta\bar{C}=\frac{\sum_{i=1}^{m}\Delta C_i}{m} \tag{3}$$

Where $\Delta\tilde{C}$ represents the average value of the error, ΔC_i represents the printing error of the i rd layer, and m represents the number of printed layers.

After the above analysis, the corresponding laser 3D printing quality data under different ceramic process parameters are obtained, which form the training samples to provide basic data for the establishment of the optimization model.

2.3. Ceramic parameter optimization model construction and solution based on data mining

2.3.1. Ceramic parameter optimization model.Data mining contains a variety of key algorithms, one of which is the neural network algorithm. Using this algorithm, the six ceramic process parameters and the corresponding laser 3D printing quality values obtained in the previous section are used as input and output samples, and the two are fitted after the operation of the input layer, implied layer, and output layer to establish a nonlinear functional relationship model between the ceramic process parameters and the laser 3D printing quality, i.e., the optimization model of ceramic process parameters. The specific process is as follows:

1) The data magnitudes of the six ceramic process parameters are unified, and the processing equations are as follows:

$$h_i=\frac{\tilde{h}_i}{\max\left|\tilde{h}_i\right|} \tag{4}$$

In the formula, h_i represents the ind ceramic process parameter after the quantitative processing, $\tilde{h}_i$ represents the ith ceramic process parameter before the processing, and $\max\left|\tilde{h}_i\right|$ represents the maximum value of the absolute value of the ith ceramic process parameter.

2) Setting relevant parameters

This paper uses SVR support vector regression algorithm, BP neural network, RF random forest, RBF radial basis function neural network and Kriging model five algorithms for the training of screw extrusion printing ceramic process parameters.

(1) SVR support vector regression algorithm. The support vector regression algorithm (SVR) applies the similar technique of support vector machine (SVM) for regression analysis, introduces the kernel function, replaces the inner product operation in the decision function with the kernel function, transforms it into a linear classification problem in a certain high-dimensional feature space by a nonlinear transformation, learns the linear support vectors in the high-dimensional feature space, selects the appropriate kernel function $K(x,z)$ and the penalty factor $C>0$, and constructs and solves the convex quadratic programming problem [21-22]:

$$\min_{w,w_0,\delta_i} \frac{1}{2}\|w\|^2 + C\sum_i \delta_i$$
$$s.t. y_i\left(w\Phi\left(x_i\right)+w_0\right) \geq 1-\delta_i \delta_i \geq 0 \tag{5}$$

At this point, the solution to the SVR regression model is:

$$f\left(x\right)=\sum_{i=1}^{N}\left(\hat{\alpha}_i-\alpha_i\right)K\left(x_i,x\right)+b \tag{6}$$

where $\hat{\alpha}_i$ and α_i are the Lagrangian operators, b is the displacement of the hyperplane, and $K\left(x_i,x\right)$ is the kernel function, which is chosen as Gaussian kernel function in this paper:

$$K\left(x,z\right)=\exp\left(-\frac{\|x-z\|^2}{2\sigma^2}\right) \tag{7}$$

where, w, w_0 are the corresponding parameters of the hyperplane, and δ_i is the relaxation variable. $\left(x_i,y_i\right)$ is the training sample, according to the obtained experimental data, in the training model of this paper, x_1, x_2, x_3 are the input variables CF content, print temperature, screw speed, and y_1 is the predicted output variable extrusion volume.

(2) BP Neural Network. BP neural network (BP) is a multilayer feed-forward neural network trained according to the error backpropagation algorithm, which generally contains three layers of the feed-forward network, i.e., the input layer, the hidden layer, and the output layer [23]. The input ceramic process parameters are weighted, and the activation function is transformed in the hidden layer to output the predicted values. Then, the gradient descent method is used to calculate the error between the predicted values and the actual values to adjust the weights of each layer of the BP neural network in the reverse direction to make the predicted values gradually approximate the actual values. In this paper, a single hidden layer neural network structure is used.

Because there are three main ceramic process parameters for screw extrusion in this paper, the results that need to be predicted are the extrusion volume under different ceramic process parameters, so the number of corresponding input layer neurons is 3, the input variables x_1, x_2, x_3 corresponding to the three ceramic process parameters of CF content, printing temperature and screw speed respectively, the number of neurons in the output layer is 1, the output variable y_1 corresponds to the predicted extrusion volume, and the number of neurons in the hidden layer is determined according to the empirical formula $\sqrt{m+n+a}$, wherein m and n are the number of neuronal nodes in the input and output layers respectively, and a is 0~10, by optimizing the training model, it is finally determined that the error value of the prediction result is the smallest when the hidden layer neuron is 7 at $a=5$.

(3) RF Random Forest Algorithm. The random forest (RF) regression model builds multiple decision trees that are not related to each other by randomly extracting samples and features, and obtains the prediction results through parallelism [24]. Each decision tree can produce a prediction result from the extracted samples and features, and the regression prediction result of the whole forest is obtained by averaging the results of all trees together, Figure 1 shows the structure of the random forest algorithm.

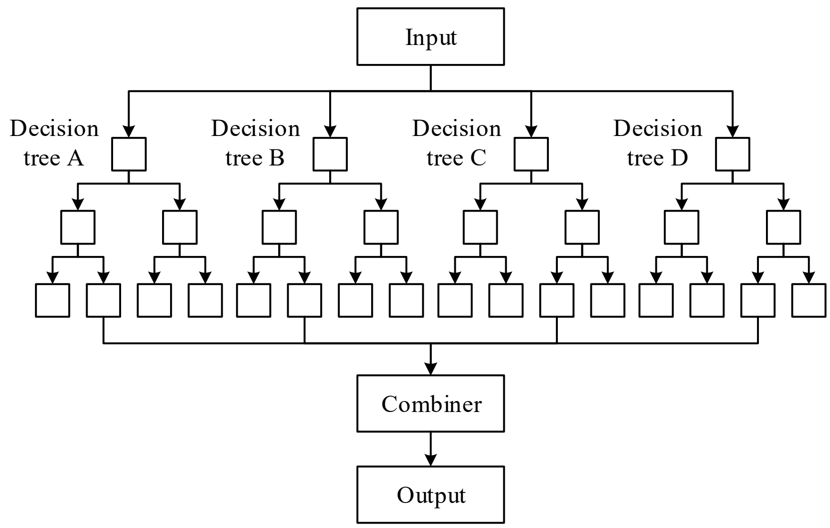

Fig. 1. Stochastic forest algorithm structure

The Random Forest Algorithm program in Matlab was called, with CF content, print temperature and screw speed as inputs and extrusion volume as output. By bringing the obtained experimental values into training and optimizing the parameters, the number of RF random forest decision tree is set to 200 and the minimum number of leaves is 3. At this time, the obtained prediction results are closest to the actual values.

(4) RBF radial basis neural network. Radial basis function (RBF) is a scalar function that is symmetric along the radial direction, and the radial basis function neural network is a single hidden layer feedforward neural network, which uses the radial basis function as the neuron activation function in the hidden layer, while the output layer is a linear combination of the outputs of the neurons in the hidden layer [25].

The learning algorithm for RBF networks generally consists of two distinct phases: the phase of determining the center of the hidden layer radial basis function and the phase of learning to adjust the radial basis function weights. Given N set of input/output sample data x_p/d_p, $p=1,2,\cdots,N$, the objective function is:

$$J(t)=\frac{1}{2}\sum_{p=1}^{N}\left\|d_p-y_p\right\|^2=\frac{1}{2}\sum_{p=1}^{N}\sum_{k=1}^{o}\left(d_{kp}-y_{kp}\right)^2 \tag{8}$$

where O is the output dimension of the output layer, d_p is the output vector of the network, and the purpose of learning is to make $J\le\varepsilon$, when the training error reaches the target, the predicted extrusion volume is output. In this study the input variable x_p is the ceramic process parameters, x_1, x_2 and x_3 correspond to CF content, printing temperature and screw speed, respectively, and the output variable d_p is the prediction result and d_1 is the predicted extruded volume.

(5) Kriging Kriging model. The Kriging Kriging model prediction method is an interpolation method based on optimal, unbiased linear prediction. It mainly relies on the spatial autocorrelation properties of the data, especially the semivariance function (or known as the variance function) to make predictions.

The Kriging prediction mathematical model includes a regression part and a stochastic part:

$$y(x)=f^T(x)\beta+Z(x) \tag{9}$$

For any prediction point x, the predicted mean $\mu(x)$ and predicted variance $\sigma^2(x)$ obtained by the Kriging model are, respectively:

$$\mu(x) = f^T(x)\beta + r^T(x)R^{-1}(y - F\beta) \tag{10}$$

$$\sigma^2(x) = \sigma^2 - 1 - r^T(x)R^{-1}r(x) + u^T(x)\left(F^T RF\right)^{-1} u(x)\Big] \tag{11}$$

where R is the correlation matrix, $r(x) = \left[R(x, x_1), \cdots, R(x, x_k)\right]$, $u(x) = F^T R^{-1} r(x) - f(x)$.

$f(x)$ is a vector of regression polynomial basis functions, β is a vector of polynomial parameters, and $Z(x)$ is a stochastic process obeying a normal distribution. x is the input ceramic process parameters, x_1, x_2 and x_3 correspond to the three ceramic process parameters CF content, printing temperature and screw speed, respectively, and $y(x)$ is the predicted extrusion volume. The dacefit function in the MatlabDACE toolbox is called to generate the Kriging model, and the three parameters $theta$, lob, and upb are set to generate the Kriging model, where $theta = [50, 50, 50]$, $lob = \left[1e^{-1}, 1e^{-1}, 1e^{-1}\right]$, and $upb = [20, 20, 20]$.

3) The six ceramic process parameters processed by the unified scale were used as inputs and $\Delta\bar{C}$ as outputs.

4) Perform implied and output layer operations with the following equations:

$$\text{Im}\,plicit\ layer: Q_i = f\left(\sum_{j=1} w_{ij}x_j - u_{ij}\right) \tag{12}$$

$$Output\ Layer: P_i = f\left(\sum_{k=1} w_{ik}Q_i - u_{ik}\right) \tag{13}$$

where w_{ij} and w_{ik} represent the connection weights between the input, implicit, and output layers, x_j represents the input layer inputs, and u_{ij} and u_{ik} represent the connection thresholds between the input, implicit, and output layers.

5) Calculate the difference ΔG between the actual output $\Delta\bar{C}'$ and the pre-input $\Delta\bar{C}$ and compare it with the error limit g.

6) When ΔG is greater than g, back-propagation is performed and the neural network parameters are adjusted until ΔG is less than g.

After the above training, the nonlinear mapping relationship model between ceramic process parameters and laser 3D printing quality, i.e., the optimization model, is established.

2.3.2. Model solving.The above trained neural network-based model of the nonlinear mapping relationship between ceramic process parameters and laser 3D printing quality was used as the objective function. Input the six ceramic process parameters used for actual testing, and utilize the trained neural network to derive the predicted values as individual fitness values. The range of values of the parameters is used as constraints. The firefly algorithm is utilized to solve the model to obtain the $\Delta\bar{C}$ minimum value and the optimal solution for the corresponding laser 3D printing ceramic process parameters. Figure 2 shows the model solution process.

The distance between feasible solutions is calculated as follows:

$$D_{ij}(M) = \left\|S_i(M) - S_j(M)\right\| \tag{14}$$

where $S_i(M)$ and $S_j(M)$ represent the positions of firefly i and firefly j, $D_{ij}(M)$ represents the distance between feasible solutions x_i and x_j at the M th iteration, and M represents the number of iterations.

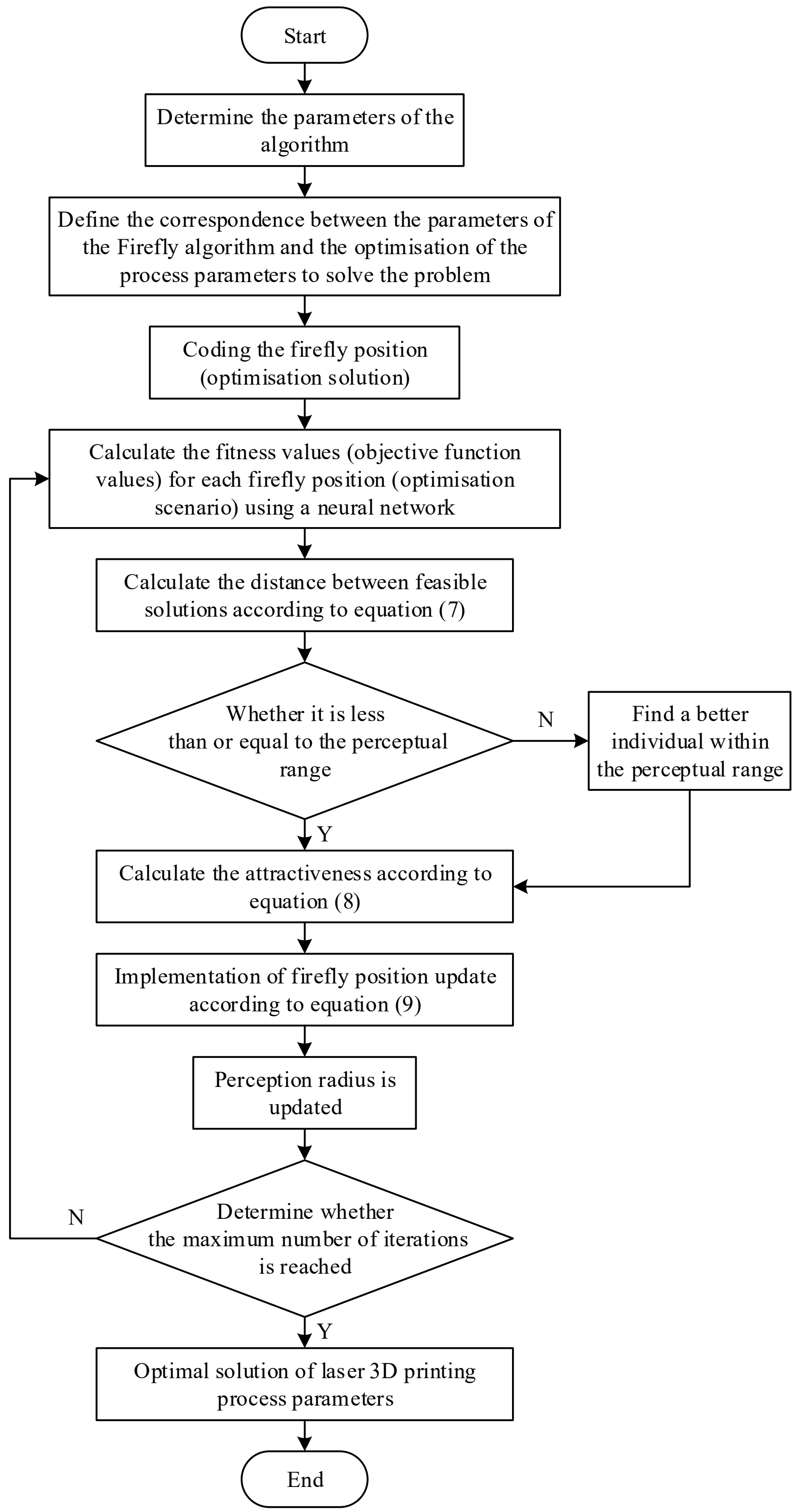

Fig. 2. Model solution process

The formula for calculating attractiveness is as follows:

$$R_{ij}(M) = R'_{ij}(M)\exp\left[-\lambda D_{ij}(M)\right] \tag{15}$$

where $R_{ij}(M)$ represents the attraction of x_i to x_j at the M nd iteration, $R'_{ij}(M)$ represents the maximum attraction, and λ represents the fluorescein update rate.

The fluorescein brightness value is calculated by Eq:

$$\psi_i(M)=(1-\gamma)\psi_i(M-1)+\lambda\cdot V_i(M) \tag{16}$$

where $\psi_i(M)$ and $\psi_i(M-1)$ represent the fluorescein values of the ird feasible solution at the M th and $M-1$th iterations, respectively, $V_i(M)$ represents the objective function value of the ith feasible solution at the P th iteration, and γ represents the fluorescein attenuation factor.

After the above analysis, the optimization study of laser 3D printing quality ceramic process parameters is completed.

3. Analysis of the design effect of personalized ceramic artwork based on 3D printing technology

3.1. Ceramic color emotional utility value analysis

3.1.1. Direct data acquisition.With the progress of science and technology, the selection of evaluation methods has become more and more scientific in evaluating color mood potency. From the “relative objectivity” of semantic scale scoring, it gradually develops into the “absolute objectivity” of physiological monitoring. Applying the model designed in this paper to personalized ceramic art design and evaluating the emotional utility value of ceramic color, we believe that this digital research method also has a lot of research space in ceramic color quantitative research. Some similar color emotional factors such as warmth, activity, and calmness were obtained for the ceramic artworks designed using this paper's method. Figure 3 shows the ceramic emotional potency data measurement; it can be seen that the ceramic color designed in this paper makes the user produce a positive emotion is dominated by positive emotions, producing 235 positive emotions, while the negative emotions are 163, positive emotions dominate, accounting for nearly 60%.

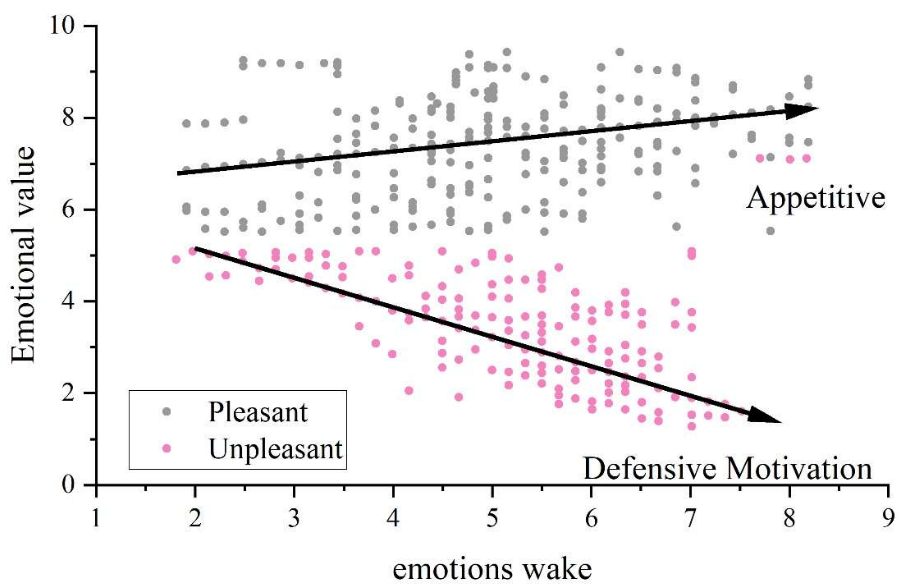

Fig. 3. The ceramic emotional value data is taken

3.1.2. Ceramic color quantification. According to the elemental chromaticity data obtained by the Konica Minolta spectrophotometer, the color characteristics are classified and counted in accordance with the real ceramic colors that are not affected by light and environmental factors, and the histograms of L, A, and B values are established. Figure 4 shows the results of the ceramic spectral chromaticity quantitative analysis; through the spectral chromaticity quantitative analysis, it can be concluded that the ceramic artwork designed in this paper has a single elemental color composition, the color luminance contrast is small, with the grey color system as the main body, and the centralized distribution of the spectral chromaticity A value (-20, -0), B value (0,20), L value (20,40), it can be illustrated that the color composition scheme of the ceramic artwork is a complete "color design system," the user experience feels good.

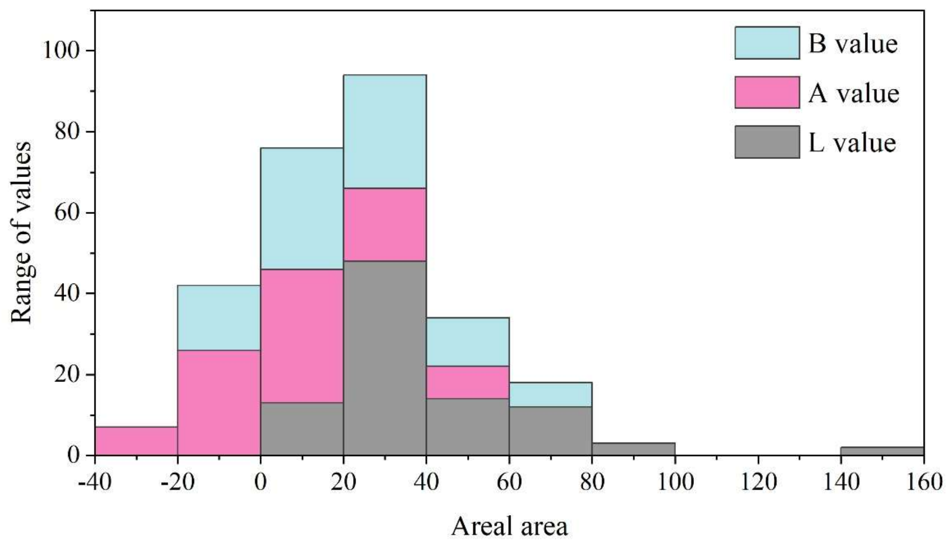

Fig. 4. The results of the analysis of the color of ceramic spectra

3.2. Personalized ceramic artwork material quality

3.2.1. Quality analysis of ceramic artwork materials. Figure 5 shows the load-displacement curve of a 3D printed ceramic core, Figure (a) for group A, (b) for group B, and (c) for group C. For the three specimens in sequence A, the specimens are in the elastic stage within the displacement of 0-4mm, and the stiffness is gradually degraded within 4-16mm. The load-carrying capacity grows slowly until it is unchanged, which belongs to ductile damage. For the three specimens of sequence B, the specimens are in the elastic stage in the displacement 0-6mm; the stiffness is highly degraded in the 6-16mm, the bearing capacity increases slowly, and a slight softening section appears, which is ductile damage. The five specimens of sequence C were damaged when the peak load was reached, the bearing capacity decreased rapidly, and brittle damage was produced. There was a multi-stage damage pattern in specimens C3-C5, and after the peak bearing capacity was reached, the specimens still maintained a certain bearing capacity, and secondary stiffness existed.

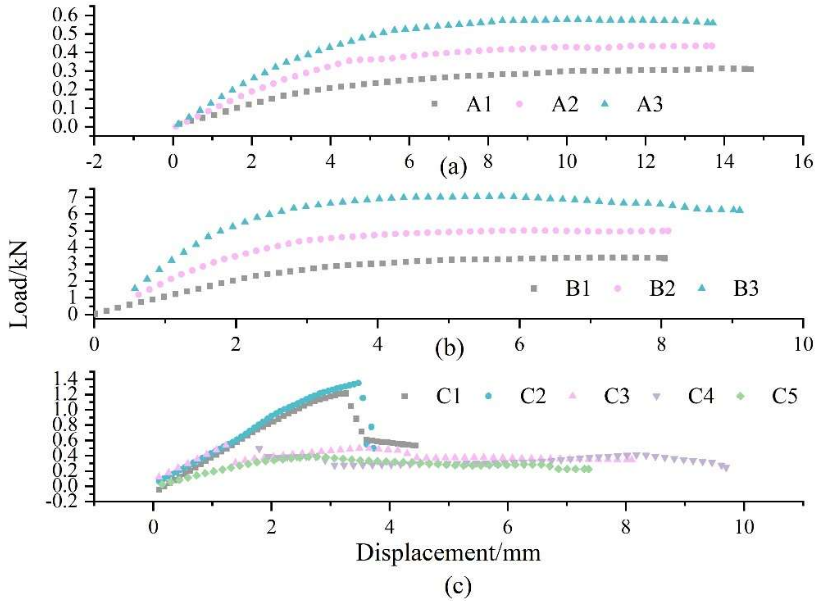

Fig. 5. 3d print clip core load displacement curve

3.2.2. Test result data.The test results of the 11 specimens were summarized, and the data were normalized for control analysis. The stiffness and load-carrying capacity were normalized against the mass and the core mass, respectively. Table 1 shows the normalization of the 3D-printed ceramic core test data. It was found that the ceramics' core configuration significantly affected the ceramics' initial stiffness, load carrying capacity, and damage mode. After the optimization of the process parameters of the ceramic core, the normalized values of the stiffness and bearing capacity mass were improved by 0.01227 and 0.0629, respectively. The quality of the specimens in the rest of the parts of the specimen was improved to different degrees, which shows that the quality of the ceramic artwork designed by the personalized ceramic 3D printing technology proposed in this paper is guaranteed.

Table 1. 3D printing clip core beam test data normalization processing

No.	Initial stiffness	Peak bearing capacity	Peak shift	Stiffness is normalized to mass	The load is normalized to the quantity	The stiffness is normalized to the quality of the sandwich	The bearing capacity is normalized to the quality of the sandwich
A1	0.064	0.315	12.456	0.00258	0.01256	0.01485	0.07546
A2	0.091	0.458	11.485	0.00345	0.01685	0.01563	0.05145
A3	0.166	0.598	8.645	0.00485	0.02482	0.01169	0.05987
B1	0.098	0.425	11.766	0.00642	0.01584	0.01861	0.06154
B2	0.176	0.636	8.055	0.00846	0.01795	0.01548	0.06174
B3	0.248	0.925	6.845	0.01665	0.02655	0.01545	0.07996
C1	0.435	1.285	3.245	0.01875	0.03245	0.05874	0.15765
C2	0.485	1.385	3.315	0.01698	0.04488	0.05364	0.05265
C3	0.563	0.598	1.325	0.01652	0.05748	0.04887	0.08746
C4	0.358	0.545	1.945	0.01355	0.02486	0.05348	0.04975
C5	0.198	0.388	2.625	0.00789	0.01875	0.02898	0.04893

3.3. Personalized ceramic art design user preference analysis

3.3.1. Questionnaire data design.Using the model designed in this paper, these personalized ceramic artwork design solutions were generated for users to analyze user preferences.

3.3.2. Mean value of user preference evaluation degree.To more comprehensively obtain the user's preference, this paper adds a questionnaire based on the design of ceramic artwork to subjectively test the user. The six user preference evaluation degrees under the user preference evaluation index and six ceramic samples combined also exclude the influence of color factors, according to the Likert five-level scale method of questionnaire production, so that the user in the browsing target ceramic samples, the five evaluation dimensions of the 11 evaluation indexes for the score, the questionnaire subject to the 32 test subjects.

Table 2 shows the user preference evaluation degree mean value, aesthetic degree score for the average of Q1 and Q2, the applicability of the score for the average of Q3 and Q4, cultural perception for the average of Q5, Q6 and Q7, the value of the score for the average of Q8 and Q9, novelty for the average of Q10 and Q11, Q1-Q11 represent a sense of coordination and balance with change and unity, sparse and dense rhythm and rhythm, decorative sense, plasticity Q1-Q11 represent a sense of harmony and balance with variation and unity, rhythm and rhythm with density and sparseness, a strong sense of decoration, plasticity, embodiment of the characteristics of traditional craftsmanship, symbolic significance, the ability to trigger emotional resonance, textured materials, subtlety and finesse, personalized morphological features, and unique textural expressions. The table shows that the mean value of the user's preference evaluation degree ranges from 2.8 to 3.5, in which the ceramic samples 4, 6, and 1 have higher ratings, respectively 3.4142, 3.3106, and 3.0556.

Table 2. User preference evaluation mean

Sample	Molding A	Structure B	Texture C	Aesthetics	Degree of application
1	A_1	B_1	C_1	2.975	3.048
2	A_1	B_2	C_2	2.725	3.078
3	A_2	B_1	C_2	2.632	3.248
4	A_2	B_2	C_3	3.245	3.648
5	A_3	B_1	C_1	3.178	3.521
6	A_3	B_2	C_3	3.185	3.485
	Culture	Value	Novelty	Means	/
1	3.015	2.825	3.415	3.0556	
2	2.632	2.931	3.125	2.8982	
3	2.988	2.415	3.526	2.9618	
4	3.215	3.248	3.715	3.4142	
5	3.248	3.078	3.425	3.29	
6	3.018	3.368	3.497	3.3106	

3.3.3. User-perceived bias values for design features.Table 3 shows the user-perceived bias values of the design features. The design features with the highest combinations of aesthetics, applicability, cultural perception, value, and novelty are $A_3B_1C_3$, $A_3B_2C_2$, $A_1B_3C_2$, $A_2B_3C_1$, and $A_2B_3C_3$. The ranking of user's perceived preferences shows that aesthetics and cultural perception are the two factors that are more important to users, and B_1 has higher aesthetics and cultural perception than B_2, 3.487>3.379,3.085>2.935, so B_1 is a better choice. Taken together, based on the results of the questionnaire survey, $A_3B_1C_3$ is the best combination of features for the target audience.

Table 3. Design characteristic user perception bias evaluation

User preference	Design feature		
	Outline A	Structure B	Texture C
aesthetics	2.848	3.487	3.014
	2.948	3.379	2.745
	3.158	3.315	3.615
Degree of application	3.385	2.755	3.185
	3.416	3.165	3.526
	3.487	3.014	2.745
Cultural perception	3.025	3.085	2.915
	3.021	2.935	3.215
	2.834	3.156	3.185
value	2.853	3.455	3.148
	3.145	3.385	2.985
	2.945	3.481	2.615
novelty	3.315	3.416	3.285
	3.658	3.048	3.315
	3.415	3.546	3.584

Ceramic samples of user preference evaluation of the average value plotted as a box plot, as shown in Figure 6, the highest degree of user preference is sample 4 (3.425), followed by sample 6 (3.245) and sample 1 (3.148), the lowest is sample 3 (2.785) and sample 2 (2.915). By observing Sample 4, it can be seen that its texture is a natural bionic form, with lines flowing gracefully like ocean waves, sparse and dense, with changes and unity, forming a calm and soothing visual effect. Observing sample 6 shows that its texture is naturally bionic, twisting and turning like a blooming flower, showing exuberant vitality. Sample 1's skeletonized structure gives it a strong sense of lightness. Sample 2's solid structural shape makes it slightly heavy, and the overall user preference rating is low. For Sample 3, the polygonal geometric contour, sharp edges, and uneven texture can easily create a sense of insecurity and vulnerability to injury, so the overall user preference is low. The combined results of the questionnaire survey show that the combination of design forms that meet the preference of the target user group is $A_3B_1C_3$, i.e. organic curved contours, skeletonized structures, and natural organic texture combinations.

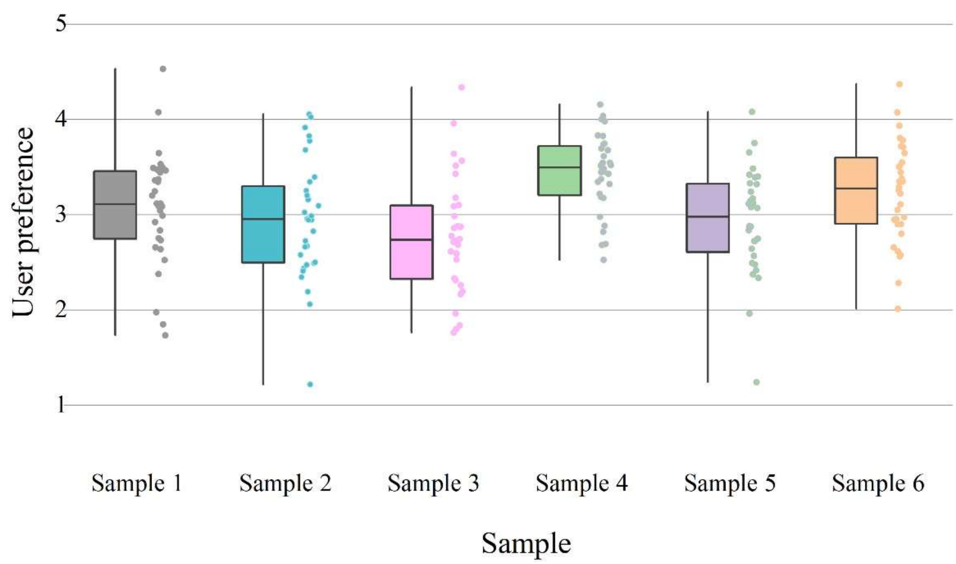

Fig. 6. User preference evaluation overall value

4. Conclusion

Based on the personalized design strategy of ceramic artwork, this paper uses 3D printing technology to determine the parameters of ceramic artwork design, obtains ceramic artwork data, constructs a ceramic parameter optimization model based on data mining algorithm, and solves the model to complete the design of ceramic artwork under 3D printing technology. Example analysis of the designed personalized ceramic artwork to explore its design effect:

1) The color of the ceramic artwork designed in this paper makes the user produce positive emotions, generating 235 positive and 163 negative emotions, which shows that the ceramic artwork designed in this paper is dominated by positive emotions, accounting for nearly 60%.

2) After the parameter optimization of the design process of ceramics, the quality normalized values of core stiffness and bearing capacity of the ceramics printed by 3D printing technology after the enhancement are 0.01227 and 0.0629 respectively, and the rest of the parts have been enhanced to varying degrees, and the ceramics are of better quality.

3) The mean values of the users' preference ratings range from 2.8 to 3.5, with ceramic samples 4, 6, and 1 having higher ratings of 3.4142, 3.3106, and 3.0556, respectively.

References

[1] Mitsouras, D., & Liacouras, P. C. (2017). 3D printing technologies. 3D printing in medicine: a practical guide for medical professionals, 5-22.

[2] Fan, D., Li, Y., Wang, X., Zhu, T., Wang, Q., Cai, H., ... & Liu, Z. (2020). Progressive 3D printing technology and its application in medical materials. Frontiers in pharmacology, 11, 122.

[3] Bozkurt, Y., & Karayel, E. (2021). 3D printing technology; methods, biomedical applications, future opportunities and trends. Journal of Materials Research and Technology, 14, 1430-1450.

[4] Ramya, A., & Vanapalli, S. L. (2016). 3D printing technologies in various applications. International Journal of Mechanical Engineering and Technology, 7(3), 396-409.

[5] Khosravani, M. R., & Reinicke, T. (2020). On the environmental impacts of 3D printing technology. Applied Materials Today, 20, 100689.

[6] Su, A., & Al'Aref, S. J. (2018). History of 3D printing. In 3D printing applications in cardiovascular medicine (pp. 1-10). Academic Press.

[7] Kamran, M., & Saxena, A. (2016). A comprehensive study on 3D printing technology. MIT Int J Mech Eng, 6(2), 63-69.

[8] Sahana, V. W., & Thampi, G. T. (2018, January). 3D printing technology in industry. In 2018 2nd International Conference on Inventive Systems and Control (ICISC) (pp. 528-533). IEEE.

[9] Besklubova, S., Skibniewski, M. J., & Zhang, X. (2021). Factors affecting 3D printing technology adaptation in construction. Journal of Construction Engineering and Management, 147(5), 04021026.

[10] Madla, C. M., Trenfield, S. J., Goyanes, A., Gaisford, S., & Basit, A. W. (2018). 3D printing technologies, implementation and regulation: An overview. 3D printing of pharmaceuticals, 21-40.

[11] Gökçe, C., & Feyzoğlu, E. (2024). A GENERAL OVERVIEW OF PORTRAIT WORKS ON CERAMIC SURFACES. Turkish Online Journal of Design Art and Communication, 14(3), 763-784.

[12] Hua, L., & Bowen, P. (2021, January). Application of Ceramic 3D Printing Technology in Modern Ceramic Manufacturing. In 2021 7th International Symposium on Mechatronics and Industrial Informatics (ISMII) (pp. 160-163). IEEE.

[13] Onal, P. B. (2012). Op-art and personal practices in contemporary ceramic art. Procedia-Social and Behavioral Sciences, 51, 655-661.

[14] Ji, Y., Zhong, S., Cai, Y., Lin, J., & Li, Z. (2023, November). An Immersive Embodied Interaction Artwork of Cantonese Porcelain. In Proceedings of the Eleventh International Symposium of Chinese CHI (pp. 361-366).

[15] Graves, M. S., Miller, S., Odundo, M., & Parry, V. (2023). Ceramic Art. Princeton University Press.

[16] Li, L. (2024, March). Application of visual aesthetic feeling of intelligent computer color in ceramic art design. In Second International Conference on Physics, Photonics, and Optical Engineering (ICPPOE 2023) (Vol. 13075, pp. 446-453). SPIE.

[17] Sun, X., Liu, X., Yang, X., & Song, B. (2021). Computer-aided three-dimensional ceramic product design. Computer-Aided Design and Applications, 19(S3), 97-107.

[18] Zhang, W., Huang, H., & Qiu, M. (2020, August). Design and implementation of virtual pottery space based on ceramic cloud service platform. In 2020 7th IEEE International Conference on Cyber Security and Cloud Computing (CSCloud)/2020 6th IEEE International Conference on Edge Computing and Scalable Cloud (EdgeCom) (pp. 145-150). IEEE.

[19] Tan, B. (2024, January). Application of 3D Printing Technology in Ceramic Product Design. In Proceedings of the First International Conference on Science, Engineering and Technology Practices for Sustainable Development, ICSETPSD 2023, 17th-18th November 2023, Coimbatore, Tamilnadu, India.

[20] Shan, X., & Yan, J. (2024). Research on the Design of Ceramic Cultural and Creative Products under the Background of Digital Technology. environmental protection, 6(5), 42-46.

[21] Mohammad Sadegh Alizadeh Gharaei,Yousef Ramezani & Mohammad Nazeri Tahroudi. (2024). Toward coupling of nonlinear support vector regression and crowd intelligence optimization algorithms in estimation of suspended sediment load. Applied Water Science(9),192-192.

[22] Yanjun Ou,Yu Cai,Lianjie Zeng,Wei Zhao & Yangyang Chen. (2024). A teaching-learning-based optimization algorithm for reliability analysis with an adaptive penalty coefficient. Structures106695-.

[23] Nai Hao Zheng,Wei Ping Zhang,Yong Zhou & Yang Liu. (2024). Confinement strength prediction of corroded rectangular concrete columns using BP neural networks and support vector regression. Structures107021-107021.

[24] Ying Yan,Jianqiang Sun,Chenglong Yu,Xiaorong Sun,Edmond Qi Wu,Tao Li... & Adrian David Cheok. (2024). An unknow fault diagnosis Scheme: A novel random deep forest for fault diagnosis of HVACs. Energy & Buildings114660-114660.

[25] Despina Karamichailidou,Georgios Gerolymatos,Panagiotis Patrinos,Haralambos Sarimveis & Alex Alexandridis. (2024). Radial basis function neural network training using variable projection and fuzzy means. Neural Computing and Applications(prepublish),1-15.